VOL. 20, NO. 20, OCTOBER 2025 ISSN 1819-6608
ARPN Journal of Engineering and Applied Sciences

www.arpnjournals.com

3D MODELLING OF STEEL CORROSION IN ALKALINE CHLORIDE SOLUTIONS: THERMODYNAMIC-KINETIC ANALYSIS OF $HFEO_2^-$SPECIATION

Suhaila Salleh[1,2] and Noor Mirza Syamimi Mortadha[3]
[1]Fakulti Teknologi dan Kejuruteraan Mekanikal, Universiti Teknikal Malaysia Melaka, Hang Tuah Jaya, Durian Tunggal, Melaka, Malaysia
[2]Centre for Advanced Research on Energy, Universiti Teknikal Malaysia Melaka, Hang Tuah Jaya, Durian Tunggal, Melaka, Malaysia
[3]Department of Mechanical and Manufacturing Technology, Kolej Vokasional Datuk Seri Mohd Zin, Alor Gajah, Melaka, Malaysia
E-Mail: suhaila@utem.edu.my

ABSTRACT

Corrosion of steel in alkaline media, with the presence of chloride, causes a very complex electrochemical behaviour. This phenomenon is governed by the speciation of iron during corrosion evolution, the formation of passive film, the formation of salt film, and chloride-induced breakdown. This study develops a thermodynamic–kinetic three-dimensional geometric model for the ferrite ion $HFeO_2^-$, a key species in alkaline conditions, and evaluates its influence on steel corrosion at pH 8, 10, and 12 in chloride-containing solutions. The model integrates equilibrium speciation through hydrolysis and oxidation equilibria, Pourbaix diagram data for Fe-H_2O systems, the dynamic concentrations of ionic species, and their kinetics into and out of a corroding pit. The results show that at pH 8, $HFeO_2^-$ concentration is negligible, and steel remains prone to active dissolution intensified by the presence of chloride. Partial stabilization of $HFeO_2^-$ occurs at pH 10, enhancing passivity, even though chloride ions significantly reduce film stability. At pH 12, $HFeO_2^-$ is thermodynamically stable, supporting the development of a strong passive layer. These findings are aligned with published pitting models in alkaline environments and highlight the central role of $HFeO_2^-$ in mediating steel durability under alkaline-chloride conditions.

Keywords: corrosion, model, steel.

Manuscript Received 16 September 2025; Revised 9 January 2026; Published 20 January 2026

1. INTRODUCTION

Steel, renowned for its high strength, cost-effectiveness, and versatility, remains the most widely used metal in construction equipment and manufacturing materials. Having these qualities, steel is still susceptible to corrosion when exposed to an aggressive environment, particularly in the presence of water and aggressive ions such as chloride. These conditions are frequently encountered in equipment exposed marine environment, which is subject to chloride ingress over time [1] [2]. Hence, it is critical to understand the corrosion science that can show the interplay between ionic speciation, electrochemical reactions, and passive film stability for predicting and mitigating steel degradation. In alkaline conditions, steel develops protective films composed primarily of Fe(III) and Fe(II) oxides and hydroxides. The stability of these films is often represented using the Fe-H_2O Pourbaix diagram, where species such as $Fe(OH)_2$, FeOOH, and the ferrite ion $HFeO_2^-$ appear as stable phases [3] [4]. Ferrite ion, also known as ferric oxyhydroxide anions, is one of the key ionic species involved in iron corrosion. The $HFeO_2^-$formation reflects the hydrolysis and formation of Fe(III) in alkaline environments, and its stability is strongly dependent on solution pH and electrochemical potential [6] [7]. At higher-ranged pH environments above pH 10, $HFeO_2^-$ plays an important role in the development of protective passive films. This inhibits further metal dissolution. Whereas in lower alkaline environments, its concentration is limited, which supports active corrosion [8] [9]. However, this balance becomes complicated with the presence of aggressive ions such as chloride, and chloride is known to promote localized breakdown [1] [10].

Experimental corrosion studies of steel have relied heavily on electrochemical processes. Undeniably, these works provide valuable empirical understandings. However, limitations occur in finding the resolution for the transient distribution of ionic species within localized corrosion sites such as pits [11]. Due to these limitations, researchers have been focusing on computational approaches, which include thermodynamic modelling, kinetic simulations, and finite-element electrochemical transport models, to better understand the science of corrosion [12][13]. Two-dimensional modelling work has been carried out that enables the simulation of coupled mass transport, electrochemical kinetics, and speciation in geometries that resemble real corroding pits [8] [14] [15] [16].

However, published work that focused specifically on the role of $HFeO_2^-$ is relatively scarce, even though this ion plays an important role in governing passivity and breakdown in alkaline chloride

environments, and most modelling work has concentrated on threshold values of chloride or generalized corrosion rates [1][2], whilst the stability of passive films is now being properly addressed. Clearly, this knowledge gap is essential to be addressed, due to the fact that there exists a mechanistic link between solution chemistry and the electrochemical behaviour of steel. Thus, this stage involves the prediction of $HFeO_2^-$ concentration profiles under varying pH and potential conditions.

The present study develops a 3D thermodynamic-kinetic model using the software COMSOL Multiphysics as a tool to simulate $HFeO_2^-$ speciation and its influence on the corrosion behaviour of steel immersed in alkaline chloride solutions at pH 8, 10, and 12. The model incorporates electrochemical kinetics, ionic mass transport, and potential-dependent stability domains to reproduce the dynamic evolution of species within a pit-like geometry. By comparing simulated concentration distributions with Pourbaix stability regions and literature experimental data, this work provides new insights into the role of $HFeO_2^-$ as a critical marker of passivity and corrosion resistance.

2. METHODOLOGY

2.1 Electrochemical Reactions and Kinetics

This model has eleven species that react in the aqueous alkaline solution [3] [4]. The species are:

a) Metal ion from dissolution process, Fe^{2+}
b) Hydroxyl ion, OH^-
c) Hydrogen ion, H^+
d) Iron (II) monohydroxide ion, $FeOH^+$
e) sodium ion. Na^+
f) chloride ion, Cl^-
g) iron (II) chloride ion, $FeCl^+$
h) metal ions, Fe^{3+}
i) iron (III) dioxide ion, FeO_2^-
j) iron hydroxide oxide ion, $HFeO_2^-$
k) iron (III) dichloride ion, $FeCl_2^+$

This model considered the diffusion, electro migration, and chemical reaction.

2.2 Thermodynamic Framework

Speciation of iron was calculated using equilibrium constants for Fe(II)/Fe(III) hydrolysis, hydroxide solubility products, and oxyanion formation reactions [3].

Relevant equilibria include:

Formation of Ferrite Ion: $Fe^{2+} + 2H_2O \rightleftharpoons HFeO_2^- + 3H^+$

Chloride Complexation: $Fe^{2+} + Cl^- \rightleftharpoons FeCl^+$

$Fe^{3+} + 2Cl^- \rightleftharpoons FeCl_2^+$

These reactions were coupled with the Nernst equation to account for potential–pH dependence.

The chemical reaction that occurs to produce the iron hydroxide oxide ion, $HFeO_2^-$, is as follows:

$$Fe^{2+} + 2H_2O \underset{k_{bHFeO_2^-}}{\overset{k_{fHFeO_2^-}}{\rightleftharpoons}} HFeO_2^- + 3H^+$$

The rate after applying the law of equilibrium:

Rfe2 = k_{fHFeO2}-$[Fe^{2+}][H_2O]^2$ - k_{bHFeO2}- $[HFeO_2^-][H^+]^3$

Hence, the production rate for $HFeO_2^-$ is *Rfe2.*

2.3 Kinetic Model

Pitting potential was estimated by considering chloride adsorption, lowering the stability of $HFeO_2^-$ and $Fe(OH)_3$. The model was set to run at pH values of 8, 10, and 12, with a chloride concentration of 1M and a temperature of 25 °C, whilst the electrochemical potential window is taken as −1.0 to -0.2V vs SHE.

2.4 Corrosion Model Geometry

The corrosion model was developed using COMSOL Multiphysics by applying the three-dimensional geometry that consists of two domains: the bulk solution and the corroding pit. Figure-2.1 illustrates the computational domain used in this study.

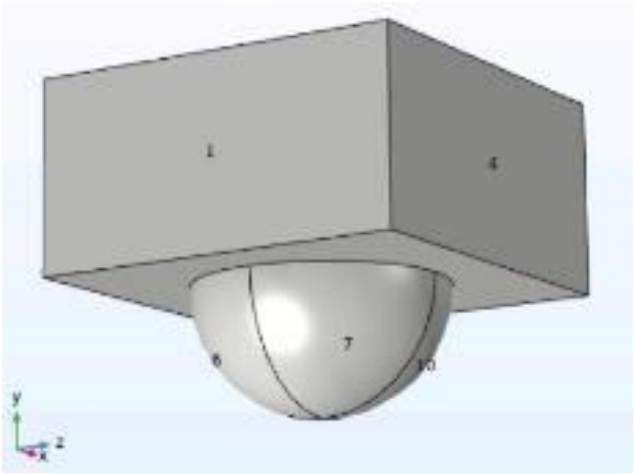

Figure-2.1. Geometry of the Corrosion Model.

Domain 1, represented by the box-shaped region, corresponds to the bulk solution surrounding the steel surface. Domain 1 acts as the bulk solution in which the metal is immersed. The mouth of the pit serves as the interface where ionic migration into and out of the pit occurs. In this region, the area is set to be void of current flow, or in other words, electrically insulated.

Domain 2 represents the pit region, which simulates the actively corroding metal. The pit was modelled with a radius of 1×10^{-6} m and a depth of 1×10^{-7} m. The lower portion of the pit (Domain 2) was defined as electrochemically active, while the upper part was set as inactive. Ionic reactions with the environment occur exclusively in the active region. The pit geometry, therefore, represents the early stage of localized attack, enabling simulation of ionic species transport and electrochemical reactions as a function of pH and applied

potential. Domain 2 was designated as the active dissolution zone where metal oxidation takes place. The total current inflow, i_{tot}, in the model is governed by the following expression:

$$i_{tot} = (J_{diss} - J_{H+}) \times F$$

Where

- F = Faraday's constant,
- J_{diss} = flux of iron dissolution (rate of Fe oxidation),
- J_{H^+} = flux of proton consumption during reduction reactions.

The dissolution of iron generates a net ionic flux, modelled through the boundary condition for Fe^{2+} as an outward flux equal to J_{diss}. The consumption of protons was expressed as an inward flux boundary condition equal to J_{H^+}. This formulation captures the coupling between iron oxidation and proton reduction within the simulated corroding pit environment.

3. RESULTS AND DISCUSSIONS

Figure-3.1, Figure-3.2, and Figure 3.3 below illustrate the concentration of $HFeO_2^-$ for pH 8, pH 10, and pH 12. The concentration of $HFeO_2^-$ in different pH solutions is presented in the three-dimensional pit geometry and plotted graph. From concentration figures and graphs plotted below show that the concentration of $HFeO_2^-$ increases as the alkalinity of the solution increases. The concentration level of $HFeO_2^-$ stays low throughout the process when it is simulated at pH 8. From Figure-3.2, at pH 10, the concentration level of $HFeO_2^-$ started to increase. However, the concentration level of $HFeO_2^-$ starts to drop to a potential of -0.45V at which the pH level starts to reduce. In caustic condition (pH12), $HFeO_2^-$ concentration level is constantly high.

3.1 Concentration of $HFeO_2^-$

An important outcome of the modelling work concerns the concentration of $HFeO_2^-$, which is a critical soluble species in alkaline environments. Figures-3.1, 3.2, and 3.3 present the spatial and temporal distribution of $HFeO_2^-$ for bulk solutions at pH 8, pH 10, and pH 12, respectively. The results are displayed both in terms of the three-dimensional pit geometry and as concentration-potential plots.

At pH 8, a clear pH dependence is observed. $HFeO_2^-$ concentration remains low throughout the simulation, with the value of 10^{-6} mol/L. This indicates that the mildly alkaline environment does not significantly stabilize this ferric hydroxo-complex. The low abundance of $HFeO_2^-$ matches the thermodynamic instability of ferric oxyhydroxide in mildly alkaline environments. This is where Fe dissolution occurs mainly as Fe^{2+}. Under these conditions, Fe tends to remain in the form of either soluble ferrous species (Fe^{2+}) or precipitated hydroxides, consistent with previous Pourbaix stability predictions [3] [15]. These results also align with Pourbaix stability predictions, which indicate that $HFeO_2^-$ becomes significant only above pH 9.5 [3] [9]. The persistence of low $HFeO_2^-$ suggests that steel in slightly alkaline environments is highly vulnerable to active corrosion, especially in the presence of chloride ions.

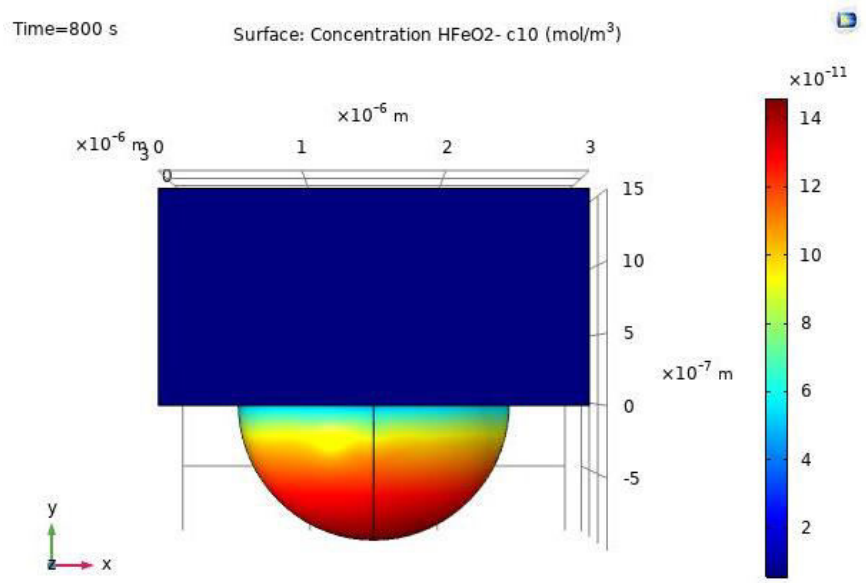

(a)

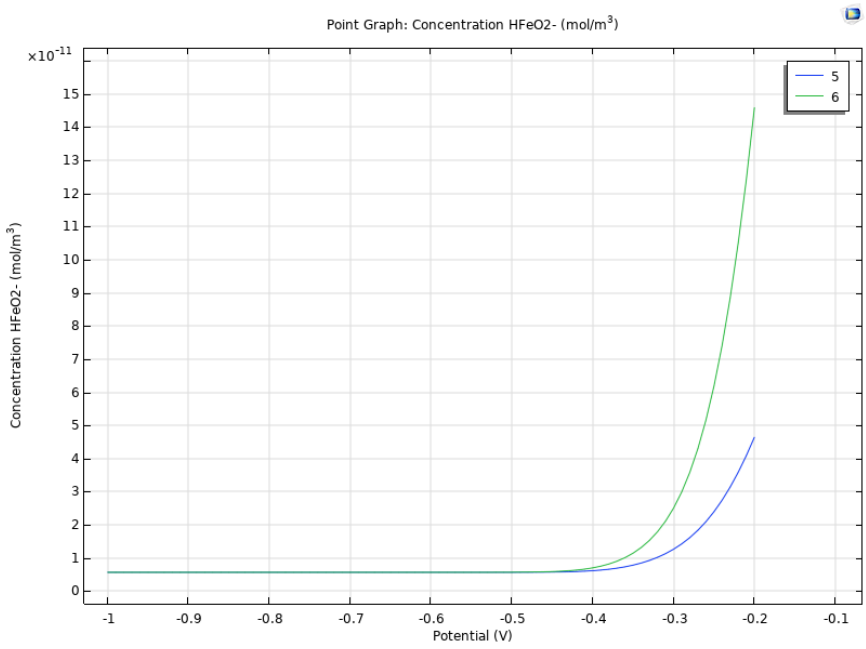

(b)

Figure-3.1. Concentration of $HFeO_2^-$ at pH 8 (a) Three-dimensional pit Geometry (b) Graph of Concentration vs. Potential.

Figure-3.2 shows that at pH 10, the concentration of $HFeO_2^-$ begins to increase, reaching values on the order of 10^{-4} mol/L. At lower potentials, the system followed a corrosion path that entered the passive region, promoting $HfeO_2^-$stabilization; thus, the rise in its concentration, where the formation of oxyhydroxide species is thermodynamically stable [6]. However, as the potential reached approximately −0.45 V, the corrosion path exited the passive region and re-entered the active domain. This causes a sharp drop in the concentration of $HfeO_2^-$ and because of dissolution processes dominating. This behaviour highlights the delicate balance between passive film stability and localized dissolution, as also emphasized in studies of passivity breakdown [10] [8].

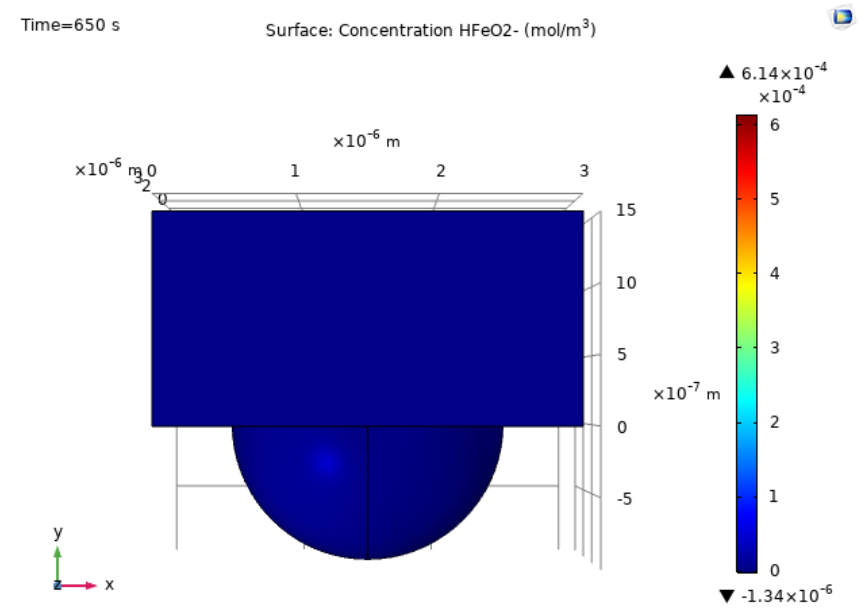

(a)

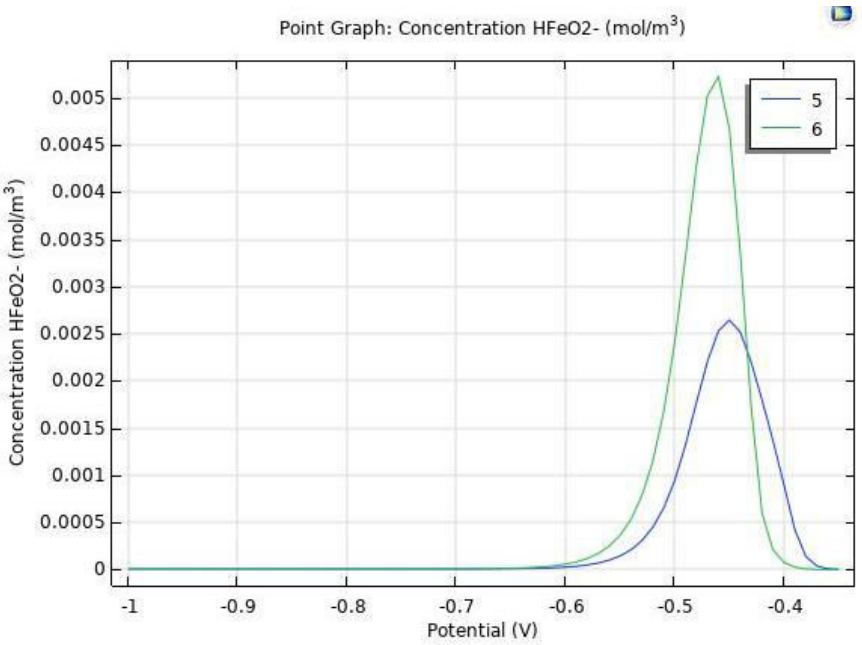

(b)

Figure-3.2. Concentration of $HFeO_2^-$ at pH 10 (a) Three-dimensional pit geometry (b) Graph of Concentration vs. Potential.

Figure-3.3 shows strongly caustic conditions of pH 12. The concentration of $HFeO_2^-$ remains consistently high throughout the simulation, approaching 10^{-3} mol/L. Under these conditions and unlike the behaviour at pH 10, the corrosion path lies entirely within the passive domain of the Pourbaix diagram, thus allowing continuous accumulation of $HfeO_2^-$ inside the pit. This indicates that the environment strongly stabilizes $HfeO_2^-$. The elevated concentration reflects the dominant equilibrium of ferric oxyhydroxide anions at high alkalinity, which not only supports the passivity of steel but also suppresses the formation of soluble ferrous ions. Such stabilization of $HfeO_2^-$ in caustic media is in line with prior electrochemical modelling work [6]. This outcome is also consistent with recent reports showing that highly caustic environments stabilize passive films through the accumulation of oxyhydroxide species, thereby suppressing active dissolution [2] [14].

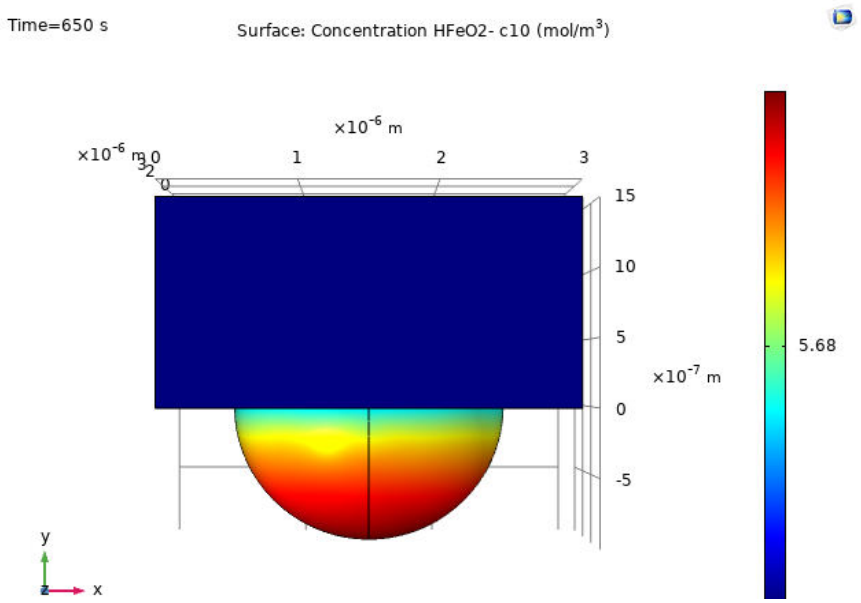

(a)

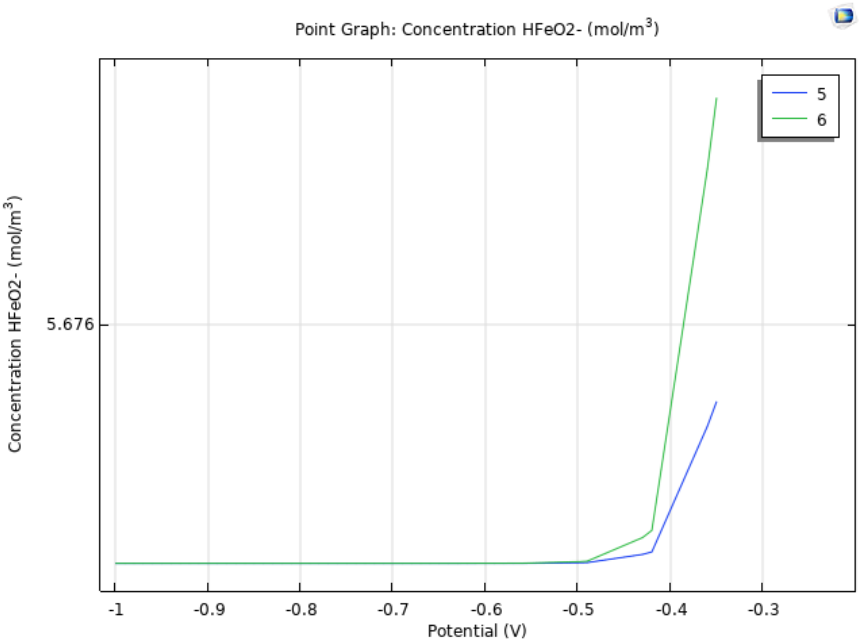

(b)

Figure-3.3. Concentration of $HFeO_2^-$ at pH 12(a) Three-dimensional pit geometry (b) Graph of Concentration vs. Potential.

Quantitatively, the modelling outcomes reveal a nearly two orders of magnitude increase in $HFeO_2^-$ concentration between pH 8 and pH 12, underscoring the importance of alkalinity in stabilizing passive films. Furthermore, the transient decrease in $HFeO_2^-$ at pH 10 near −0.45 Villustrates the sensitivity of speciation to potential-dependent stability domains. This suggests that steels exposed to environments fluctuating between near-neutral and moderately alkaline pH are at greater risk of localized breakdown, particularly in the presence of chloride ions that destabilize passive domains [7] [11].

Overall, the modelling results demonstrate that the formation and persistence of $HFeO_2^-$are strongly governed by bulk solution pH. At lower alkalinity (pH 8), the species is essentially absent, while at intermediate alkalinity (pH 10), its concentration rises but is vulnerable to reduction when the system enters the corrosion domain. Only at strongly alkaline conditions (pH 12) does $HFeO_2^-$ remain stable throughout the electrochemical process. These findings underscore the importance of solution pH in defining corrosion resistance of steel in alkaline media,

particularly in the presence of chloride ions that can trigger breakdown of passive domains.

3.2 Influence of Chloride Ions on $HFeO_2^-$ Stability

Studies have shown that the presence of chloride ions had a noticeable disrupting effect on $HFeO_2^-$ concentrations across all pH conditions. Adsorption of chloride at the pit mouth and on passive films suggests localized acidification, which shifts equilibria away from $HFeO_2^-$ stability domains [1][11].

At pH 8, the immediate impact of chloride was observed. The low concentration of$HFeO_2^-$ diminished further, and the corroding metal surface remains active. This states that near-neutral alkaline environments are unable to sustain protective ferric oxyhydroxide species once chloride is present.

At pH 10, chloride shifted the breakdown potential towards more negative values. This reduces the stability range for $HFeO_2^-$, causing the drop in $HFeO_2^-$ concentration once the potential crosses into the corrosion domain. This finding is consistent with the published work of [8]. This indicates that the chloride threshold concentration for depassivation decreases as the potential becomes more cathodic [2].

At pH 12, the level of severity of chloride effects was not high, but still significant. Even in strongly caustic solutions, high concentrations of chloride can eventually destabilize passive films regardless of alkalinity. This is consistent with the work done by Li *et al*. [14] and Zhang *et al*. [9], who reported that the presence of very high chloride concentration can lower the critical pitting potential.

3.3 Mechanistic Interpretation and Practical Implications

At intermediate alkalinity, which is at pH 10, the metal surface turns passive, where $HFeO_2^-$forms. However, as the applied potential shifts toward more negative values, the passive film becomes less stable. This destabilization is manifested in the model by a drop in $HFeO_2^-$concentration. This is likely because iron dissolution occurs, and chloride competes for binding, forming a salt film.

At around -0.45 V, which is seen in the pH 10 model, this appears to be a critical potential beyond which passive behavior cannot be sustained. This is analogous to experimentally observed passivity breakdown potentials in alkaline chloride environments [8] and chloride thresholds [2]. This model can help in predicting the thresholds and identify safe operational potentials for steel in alkaline environments with chloride present.

In terms of pH, higher pH increases the thermodynamic stability of $HFeO_2^-$. The model shows that at pH 12, the film remains passive across potentials considered, reflecting that even in the presence of chloride, the passive film is strong. This suggests that maintaining high alkalinity is an effective corrosion mitigation strategy.

3.4 Corrosion Pathways and Passivity Breakdown

The modelling results suggest that the stability of $HFeO_2^{-i}$ is related to the corrosion pathway of steel. When the metal surface is in the passive region, $HFeO_2^-$ accumulates and stabilizes the protective film. On the other hand, when the system becomes active due to chloride attack, $HFeO_2^-$ concentrations decline rapidly, reflecting the breakdown of the passive film. This correlation suggests that $HFeO_2^-$ may play a role as a mechanistic indicator for assessing chloride-induced depassivation. In reality, steels exposed to environments fluctuating between pH 8 and 10are at greater risk of localized breakdown, given that at these pH values$HFeO_2^-$ stability is highly sensitive to chloride [1][13]. Meanwhile, at pH 12, stable $HFeO_2^-$concentrations provide flexibility, although high chloride contents can still eventually trigger passivity loss.

3.5 Summary

The modelling confirms that pH control remains a primary strategy for corrosion mitigation, as alkaline conditions promote the stability of ferric oxyhydroxide species [9][1]. By explicitly resolving $HFeO_2^-$ concentration distributions in 3D geometries, this study advances beyond empirical threshold approaches and provides mechanistic insights into the conditions under which steel transitions from passive to active states. Future work should integrate these thermodynamic–kinetic simulations with experimental in situ monitoring, to validate $HfeO_2^-$ as a predictive parameter for corrosion initiation.

4. CONCLUSIONS

This study clarifies the role of ionic speciation, particularly the stability of the ferrite species $HfeO_2^-$, in governing the corrosion response of steel immersed in alkaline solutions of pH 8, 10, and 12 under the influence of chloride ions. Based on the Fe-H_2O system and Pourbaix diagram analysis, thermodynamic considerations indicate that at moderately alkaline pH 8-10, the dominant soluble species transitions from ferrous hydroxide complexes toward the ferrite ion $HfeO_2^-$. This provides passivation through the formation of iron oxide layers. Nevertheless, chloride ions promote localized breakdown of this passive layer. At pH 12, the stability domain of $HfeO_2^-$ is extended, and the passive film becomes tougher, leading to a reduced overall corrosion rate. It is suggested that the strongest passivation occurred at pH 12, although localized chloride-induced attack remained detectable. Thus, the corrosion resistance of steel in alkaline chloride environments is strongly pH-dependent, with $HfeO_2^-$ speciation acting as a critical intermediate in passive film formation and stability. Overall, the findings emphasize that higher alkalinity enhances the protective role of ferrite ions against general corrosion, but the susceptibility to chloride-induced pitting remains a limiting factor for long-term durability of steel in alkaline media.

ACKNOWLEDGMENT

This research was funded by a grant from the Ministry of Higher Education of Malaysia (FRGS Grant, No: FRGS/1/2018/STG06/UTEM/02/2). The authors would also like to thank Universiti Teknikal Malaysia Melaka (UTeM) for all the support given.

REFERENCES

[1] Angst U. 2018. Chloride-induced reinforcement corrosion in concrete-Concepts of critical chloride threshold values. *Corrosion Science*, 129, 142-155http://hdl.handle.net/11250/236720

[2] Fache V., Belec L., Nguyen V. T., *et al*. 2024. On the impact of cathodic polarization on the chloride threshold of carbon steel in alkaline solutions. Materials and Corrosion, 75(5): 493-504. https://doi.org/10.1002/maco.202414601

[3] Pourbaix M. 1974. Atlas of Electrochemical Equilibria in Aqueous Solutions. National Association of Corrosion Engineers. https://doi.org/10.1051/jp4:2006136008

[4] Salleh S. and Stevens N. 2018. A mathematical model to study the propagation of pitting corrosion in steel immersed in a chloride solution. Journal of Engineering and Applied Sciences. 13(1): 134-139.

[5] Salleh S. 2013. Modelling pitting corrosion in carbon steel materials. The University of Manchester (United Kingdom).

[6] Schwertmann U. and Cornell R. M. 2000. Iron Oxides in the Laboratory: Preparation and Characterization. Wiley-VCH.DOI:10.1002/978352761322

[7] Macdonald D. D. 2011. Passivity-the key to our metals-based civilization. Pure and Applied Chemistry, 71(6): 951-978.http://dx.doi.org/10.1351/pac199971060951

[8] Qiu J., Zhu Y., Xu Y., Li Y., Mao F. and Macdonald D. D. 2022. Effect of chloride on the pitting corrosion of carbon steel in alkaline solutions. *Journal of the Electrochemical Society*, 169, 031501DOI 10.1149/1945-7111/ac580c

[9] Zhang H., Li Y., Xu Y. and Qiu J. 2023. Electrochemical modeling of localized corrosion processes in chloride-contaminated alkaline solutions. *Corrosion Science.* 216, 111130.

[10] Frankel G. S. 1998. Pitting corrosion of metals: A review of the critical factors. Journal of the Electrochemical Society. 145(6): 2186-2198.

[11] Kelly R. G., Scully J. R., Shoesmith D. W. and Buchheit, R. G. 2003. Electrochemical Techniques in Corrosion Science and Engineering. CRC Press.

[12] Macdonald D. D. 2011. Passivity-the key to our metals-based civilization. Pure and Applied Chemistry. 71(6): 951-978.

[13] Cui Z., Guo X., Yang J. and Wu W. 2021. A review of modeling studies on the corrosion behavior of steel in concrete. Construction and Building Materials. 270, 121454.

[14] Li Y., Qiu J., Mao F. and Macdonald D. D. 2023. Modelling passivity breakdown and chloride effects in alkaline environments. Electrochimica Acta. 446, 142057.

[15] Bockris J. O'M. and Reddy A. K. N. 2000. Modern Electrochemistry, Vol. 2. Kluwer Academic/Plenum.

[16] Li Xuanpeng, Yang Zhao, Wenlong Qi, Jidong Wang, Junfeng Xie, Hairui Wang, Limin Chang *et al.* 2019. Modeling of pitting corrosion damage based on electrochemical and statistical methods. Journal of The Electrochemical Society 166, no. 15: C539 https://doi.org/10.1149/2.0401915jes

[17] Guo Peng, Erika Callagon La Plante, Bu Wang, Xin Chen, Magdalena Balonis, Mathieu Bauchy, and Gaurav Sant. 2018. Direct observation of pitting corrosion evolutions on carbon steel surfaces at the nano-to-micro-scales. Scientific reports 8(1): 7990 https://doi.org/10.1038/s41598-018-26340-5

[18] Si Wujun, Qingyu Yang and Xin Wu. 2019. Material degradation modeling and failure prediction using microstructure images. Technometrics. 61(2): 246-258. https://doi.org/10.1080/00401706.2018.1514327

[19] Jafarzadeh, Siavash, Jiangming Zhao, Mahmoud Shakouri, and Florin Bobaru. 2022. A peridynamic model for crevice corrosion damage. Electrochimica Acta. 401: 139512 https://doi.org/10.1515/corrrev-2019-0049